Accelerating seismic release from a self-correcting stochastic model

Steven C. Jaumé
Department of Geology and Environmental Geosciences, College of Charleston, Charleston, South Carolina, USA

Mark S. Bebbington
IIS&T, Massey University, Palmerston North, New Zealand

Received 28 October 2003; revised 1 September 2004; accepted 8 September 2004; published 1 December 2004.

[1] We investigate the conditions under which the "stress-release model," a stochastic version of the elastic rebound model, produces synthetic earthquake sequences characterized by Accelerating Seismic Release (ASR). In this model, the level, or "stress," of the process accumulates linearly with time through tectonic input and decreases as the result of earthquakes. These "stress drops" correspond to some power of the energy released in the earthquakes, either $E^{0.5}$ (Benioff strain) or E (seismic moment). Earthquakes occur in a point process with rate controlled by the level of the process. We hypothesize that the critical factor in the appearance of ASR is the manner in which the event sizes depend on the level of the process. This is modeled by the square root of energy released following either a tapered Pareto or truncated Gutenberg-Richter distribution, with maximum earthquake size controlled by a "tail-off" or "truncation" point. As the tail-off point becomes large, so does the average size, corresponding to an "acceleration to criticality" of the system. We found that those cases where the underlying level of the process corresponded to accumulated seismic moment produced numerous ASR sequences, whereas those cases using accumulated Benioff strain as the level did not. These results suggest that the occurrence of ASR is strongly dependent on how large earthquakes affect the dynamics of the fault system in which they are embedded, and hopefully provide some insight into the mechanics of acceleration to criticality, i.e., on the possible causes of occurrence/nonoccurrence of ASR. *INDEX TERMS:* 3220 Mathematical Geophysics: Nonlinear dynamics; 3210 Mathematical Geophysics: Modeling; 7209 Seismology: Earthquake dynamics and mechanics; 7223 Seismology: Seismic hazard assessment and prediction; *KEYWORDS:* accelerating seismic release, intermittent criticality, stochastic stress release model

Citation: Jaumé, S. C., and M. S. Bebbington (2004), Accelerating seismic release from a self-correcting stochastic model, *J. Geophys. Res.*, *109*, B12301, doi:10.1029/2003JB002867.

1. Introduction

[2] There has been a growing trend in seismology to utilize concepts from statistical physics to explain observations of the earthquake process. Observations such as the Gutenberg-Richter Magnitude-Frequency relationship and the small magnitude of dynamic stress drops relative to predicted crustal stresses have suggested to some that the seismogenic crust is constantly in a state of "self-organized criticality" (SOC), where the initiation of any small event has the potential to grow into a large earthquake that spans the full dimension of the tectonic fault system [*Kagan*, 1994; *Geller et al.*, 1997]. In contrast, the Accelerating Seismic Release (ASR) hypothesis, based on the postevent study of seismic catalogs, is that the regional rate of seismic moment or strain release accelerates prior to the occurrence of many moderate to large earthquakes in deforming continental regions [*Jaumé and Sykes*, 1999, and references therein]. A number of authors [e.g., *Sornette and Sammis*, 1995; *Rundle et al.*, 1999] have viewed this behavior as being analogous to changes in a physical system approaching a phase transition. In these so-called "intermittent criticality" models, a fault system alternately approaches and retreats from a critical state. During the approach to the critical state, there is progressive growth in long-range correlations in the underlying stress field, allowing for increasingly larger earthquake events to occur. Thus ASR can be considered a symptom of a system "accelerating to criticality."

[3] The acceleration in seismic release is most often described by a power-law time to failure equation [*Varnes*, 1989; *Bufe and Varnes*, 1993]:

$$\Omega(t) = A + B(t_f - t)^m, \tag{1}$$

where $\Omega(t)$ is the observed quantity of interest (cumulative seismic moment, Benioff strain, or event count), t_f is the

0148-0227/04/2003JB002867$09.00

Table 1. Definitions of Terms

Variable	Representation
$\Omega(t)$	Cumulative seismic release (Benioff strain or seismic moment).
A	$A = \Omega(t_f)$ in (1).
B	$B < 0$; parameter controlling increase in $\Omega(t)$ in (1).
m	$0 < m \leq 0.8$; parameter controlling curvature in (1).
t_f	Time of mainshock event (time-of-failure).
$X(t)$	Level of the underlying stochastic process.
ρ	$\rho > 0$; tectonic input rate in (3).
S_i	Stress release of the ith earthquake.
$S_i = 10^{2.4+0.75Mi}$ or $10^{9.0+1.5M_i}$	Alternative relations between stress release and magnitude.
$S(t) = \sum_{t_i<t} S_i$	Accumulated stress release from earthquakes in (3).
$\Psi(x)$	Instantaneous rate of occurrence when $X(t) = x$.
μ, ν	$\nu > 0$; parameters controlling relationship between $X(t)$ and Ψ in (4).
$\lambda(t)$	Point process intensity of the stochastic process.
$F(y)$, $F(M)$	Distribution of earthquake stress releases and magnitudes, respectively.
y_0, m_0	Lower stress release and magnitude cutoffs.
α	Parameter controlling decrease in event size frequency with magnitude in (5).
U, γ	Upper turning stress release (U) and equivalent magnitude (γ) in (5).
$\gamma = u_0 + u_1 e^X$ or $u_0 + u_1 (1 + X_+)^{u_2}$	Alternative relations between level $X(t)$ and upper turning magnitude.

time of the mainshock event that ends the sequence, and A, B, and m are parameters that describe the acceleration (a complete definition of terms used in this paper is given in Table 1). Seismic moment is often considered the preferred quantity to use on theoretical grounds [*Main*, 1999; *Vere-Jones et al.*, 2001] but Benioff strain is most often used in empirical work because it appears to provide better "post-dictions" of t_f [*Bufe and Varnes*, 1993]. We perform our analyses in section 5 using both cumulative Benioff strain and cumulative moment release, but for clarity of exposition, will present our results using Benioff strain and simply review the results using seismic moment in section 6. In terms of earthquake quantities the cumulative Benioff strain release is [*Benioff*, 1951; *Gutenberg and Richter*, 1956]

$$\Omega(t) = \sum_{i=1}^{N(t)} E_i^{1/2} = \sum_{i=1}^{N(t)} \epsilon_i = \sum_{i=1}^{N(t)} 10^{2.4+0.75M_i}, \qquad (2)$$

where $N(t)$ is the number of events in $(0, t)$, and E_i, ϵ_i and M_i are the energy release, Benioff strain release, and magnitude, respectively, of the ith event.

[4] Proper quantification of earthquake occurrence forecasts from ASR requires some way of simulating sequences of events from the model. For example, large synthetic catalogs provide the means to examine inference properties of parameter estimates, and thus obtain some idea of the expected precision of forecasts. *Vere-Jones et al.* [2001] consider simulating directly from the ASR formulation (1), identifying a spectrum of methods for doing so. However, a difficulty with the formulation of the ASR model in (1) is that it only models a single sequence, terminating in a major event. There is no indication of the mechanism between sequences. Limited observational evidence from the San Francisco Bay region is that there have been at least three such sequences between 1850 and 1989 [*Bufe and Varnes*, 1993], and thus a model that provides for repeated ASR sequences is desirable.

[5] The purpose of the present work is to propose a stochastic model capable of displaying repeated instances of acceleration to criticality, and to use this model to further define the conditions under which ASR behavior occurs. To date, most studies of this issue have been undertaken using simulated earthquake catalogs generated by various physically based computational models ranging from simple cellular automata [*Steacy and McCloskey*, 1998, 1999; *Sammis and Smith*, 1999] to those with a more elaborate physical basis [*Mora et al.*, 2000; *Ben-Zion et al.*, 2003]. While the model parameters that control the type of behavior exhibited can be clearly examined in these simulations, there is no method for estimating these from observed data. We note that even results from simulation models that are designed to produce ASR-type behavior do not always clearly exhibit a classic ASR sequence prior to all large earthquakes [e.g., *Jaumé et al.*, 2000]. Since these models generally contain a large number of interacting elements, there is always some "randomness" in the occurrence of individual earthquakes; i.e., even in a designed ASR system, the exact timing and location of the large earthquake that ends an ASR sequence need not be predictable. Since we know that ASR is not an universal phenomena, this uncertainty must be at least as prevalent in natural systems. Thus stochastic models, allowing for the quantification of this random element, are to be preferred. The additional difficulty that we do not (and may never) exactly know the state of stress in any part of the Earth's crust, reinforces this preference, as such models can embody our uncertainty regarding the state of the system.

[6] The cumulative strain release $\Omega(t)$ in (2) contains two potential sources of variation: the number of events and their average size. *Jaumé and Sykes* [1999] and *Jaumé* [2000] examined variations in earthquake frequency-magnitude distributions during known ASR sequences and found that the acceleration arises most often from an increase in the size of the events and less frequently from an increase in numbers. This leaves open the question of how the two elements interact. The hypothesis we will advance here is that in order to have "acceleration to criticality," there should be an underlying state of the system related to the "closeness to criticality" and that either or both of the rate of events and the mean magnitude increases with this underlying state. *Ben-Zion et al.* [2003] find similar behavior in a discrete simulation model of a strike-slip fault with realistic dynamic weakening;

frequency size statistics of small and moderate events evolve in time between large earthquakes, showing an increase in the event rate and the maximum event size, as a large earthquake approaches.

[7] Since we desire a model with the potential to estimate the parameters from observed data, and for the output characteristics to evolve as in (1), we are naturally led to the class of point process models with history-conditional intensities [see, e.g., *Daley and Vere-Jones*, 2003]. The simplest such model possibly suitable for our purposes is the stress release model [*Vere-Jones*, 1978]. It is primarily attractive because of the physical intuition behind the model; the intensity is an increasing function of an underlying system variable, be it accumulated elastic strain energy, accumulated seismic moment, etc. Thus cause and effect are very clear, which is not necessarily the case with more complex simulation models. If the stress-release model can produce ASR behavior, it will provide a mechanism for the evolution of the seismic record between ASR sequences, and thus assist investigation of parameter estimation and hazard forecasting using ASR models. Furthermore, as the stress-release model is a point process with a history-conditional intensity, there exists a well-defined statistical procedure for fitting the parameters to data. This may provide a useful alternative to, and a check on, the usual ASR methodology in some circumstances.

[8] This paper is an investigation of the conditions under which an elaboration of the stress release model of *Vere-Jones* [1978] produces synthetic earthquake catalogs containing repeated ASR sequences. In doing this we hope to both provide a means to simulate multiple occurrences of ASR and to gain further insight into the nature of fault systems that do and do not produce this type of behavior. We shall next describe the stress release model and how, in particular, the event rate is parameterized as a function of the earthquake history. The following section describes the distribution of the simulated event sizes, and how this can produce "acceleration to criticality." Section 4 then summarizes the experimental factors, including the dependence of the size distribution on the history of the process, and the simulation procedure. The results are presented in section 5 and discussed in the final section.

2. Stress Release Model

[9] We shall henceforth use the term "stress" to denote the quantity which is accumulated to form the underlying system variable, or level, of the stochastic process. The stress release model is a stochastic version of the elastic rebound model, where the probability of earthquake occurrence is controlled by the deterministic buildup of stress within a region and its release, stochastically, through earthquakes. Note especially that this "stress" is a scalar quantity, and not a tensor as is the true stress. It is intended to track the level of, for example, elastic strain energy or seismic moment accumulated in a large tectonic region, whereas the actual stress tensor in a region is highly heterogeneous. Further, the region size for which the stress release model is appropriate [*Zheng and Vere-Jones*, 1991, 1994] is comparable to those identified by *Bowman et al.* [1998] as exhibiting ASR behavior. For the purposes of this study we will simply assume that the region modeled by the stress release process corresponds to one exhibiting ASR behavior. Thus we abstract the spatial dimension, leaving only the temporal dimension, which can thus be modeled by the stress release process.

[10] The level of the process, $X(t)$, evolves as

$$X(t) = X(0) + \rho t - S(t), \tag{3}$$

where $X(0)$ is the initial value, ρ is a constant loading rate from external tectonic forces, and $S(t)$ is the accumulated stress release from earthquakes within the region over the period $(0, t)$, that is, $S(t) = \sum_{t_i<t} S_i$, where t_i and S_i are the origin time and the stress release associated with the ith earthquake.

[11] Earthquakes above a fixed threshold size, m_0, are assumed to occur stochastically, where the probability of an event occurring in the time interval $(t, t + \Delta)$ is $\Psi(X(t))\Delta + o(\Delta)$ for small Δ. Thus the history controls the rate of events through the current level. Obviously the function $\Psi(X(t))$ must be nondecreasing. For example, $\Psi(X(t))$ = constant results in a random (Poisson process) model of occurrences, while

$$\Psi(X(t)) = \begin{cases} 0, & X(t) \le x_c, \\ \infty, & X(t) > x_c, \end{cases}$$

corresponds to a time-predictable model, supposing a failure strength x_c. An effective compromise [*Zheng and Vere-Jones*, 1991, 1994] between these extremes of behavior is $\Psi(X(t)) = \exp[\mu + \nu X(t)]$. This can also represent the behavior that might be expected from a region with a locally heterogeneous strength. We interpret μ as representing the background seismicity rate, although this cannot be distinguished from the initial level $X(0)$ using observed data. Note that although $X(t)$ can become negative in (3), which is intuitively unattractive for a physical quantity, the inclusion of μ in the formulation means that $X(t)$ is in fact merely a perturbation relative to some unknown level. Meanwhile, the exponential form of $\Psi(X(t))$ ensures that the probability of an event remains positive. The "sensitivity" parameter ν is interpreted as an amalgam of the distribution of fault strengths in the region.

[12] Statistical analysis is made possible by treating the data in historical earthquake catalogs as a point process in time-stress space with history-dependent conditional intensity function

$$\lambda(t) = \Psi(X(t)) = \exp[\mu + \nu(X(0) + \rho t - S(t))]. \tag{4}$$

Estimates of the parameters can then be found by maximizing the log-likelihood function [see, e.g., *Daley and Vere-Jones*, 2003, section 7.2].

3. Earthquake Magnitude-Frequency Distributions

[13] Simulating events from a stochastic model requires some means of generating the size of the event, or equivalently, a probability distribution for the magnitude. While this may follow a Gutenberg-Richter power-law distribution

for small to medium magnitudes, the power-law breaks down for larger magnitudes such as those of the terminating ASR events [*Kagan*, 1991]. Also, if we are to generate a change in the rate of seismic release, we need to increase either the rate of events or their average size. The evidence from observed ASR sequences [*Jaumé*, 2000] suggests that both can occur. Generating ASR through increasing average event size in the case of the Gutenberg-Richter distribution requires decreasing the b value, but this is not feasible in simulation because of the finite possibility of generating an arbitrarily large event. Moreover, observational evidence [*Jaumé*, 2000] is that the b value of the lower magnitude part of the distribution does not change during ASR sequences. Hence we need finer control over the large magnitude tail of the distribution, in order to increase the average event size.

[14] Rather than the simple Gutenberg-Richter power law, we will use the tapered Pareto (or Kagan) [*Vere-Jones et al.*, 2001; *Daley and Vere-Jones*, 2003, section 7.3] and truncated Gutenberg-Richter distributions [*Burroughs and Tebbens*, 2002]. Both of these distributions have the property that the parameter controlling the large magnitude tail of the distribution can be linked to the level $X(t)$. We note here that theoretical discussions of the "intermittent criticality" model generally refer to changes in the magnitude distribution using the tapered Pareto model [*Rundle et al.*, 1999, 2000]. Thus we will focus our discussion upon the tapered Pareto distribution, stopping to note where the behavior of the truncated Gutenberg-Richter distribution differs.

[15] The tapered Pareto form has the distribution function (assuming that the lower curvature, corresponding to catalog incompleteness, is immaterial to our purposes and can be ignored)

$$F(y) = 1 - \left(\frac{y}{y_0}\right)^{-\alpha} \exp[-(y - y_0)/U], \qquad y > y_0. \quad (5)$$

For small and intermediate y, this is close to power-law form, but for y large it is dominated by the exponential taper. Increasing the turning point U increases the mean of the distribution, and thus the average event size. Distributions of this type are commonly used when it is desirable for the body of the distribution to approximate a power-law, but where the moments must remain finite, as is the case with earthquake sizes. For more on the distribution (5) and its properties, see *Kagan* [1991, 1997, 2002], *Vere-Jones et al.* [2001], and *Kagan and Schoenberg* [2001]. In the geophysical literature the tapered Pareto distribution usually appears as the modified Gutenberg-Richter distribution [*Sornette and Sornette*, 1999; *Bird et al.*, 2000]

$$F(M) = 1 - (M_t/M)^{\beta} \exp[(M_t - M)/M_c] \quad (6)$$

for seismic moments, where M_t is the observational completeness threshold (typically presumed known), and M_c the upper turning point.

[16] The truncated Gutenberg-Richter distribution [*Burroughs and Tebbens*, 2002] for magnitude has distribution

$$F(M) = \frac{1 - \exp[b \ln 10(m_0 - M)]}{1 - \exp[b \ln 10(m_0 - m_{\max})]}. \quad (7)$$

In this case the upper cutoff magnitude $m_{\max}$ sets a strict limit on the size of the largest event, as opposed to the "softer" upper magnitude limit of (5).

[17] In order to be compatible with the results of *Vere-Jones et al.* [2001], we will let the random variable following (5) be the Benioff strain release ϵ_i, which is then converted to magnitude as [*Benioff*, 1951; *Gutenberg and Richter*, 1956]

$$M = m_0 + \frac{4}{3} \log_{10} \epsilon_i. \quad (8)$$

Thus the "b value" in the power-law range of the distribution is equal to 0.75α, and we will specify U through the *equivalent magnitude* $\gamma = (\log_{10} U - 2.4)/0.75$. For convenience, we will also use γ as synonymous with $m_{\max}$ when referring to the truncated Gutenberg-Richter.

[18] For our purposes, the importance of (5) lies in the fact that, when $\gamma = \infty$ (i.e., there is no round-off of the distribution), the mean of the distribution is infinite for $\alpha \geq 1$. In other words, $\alpha = 1$ is the "critical value" of the distribution. Conversely, we see that if $\alpha = 1$, the mean becomes infinite in the limit $\gamma \rightarrow \infty$. Thus we can realize our hypothesis of "proceeding to criticality" (in the sense of the event size distribution) by setting $\alpha = 1$ and increasing γ as $t \rightarrow t_f$. This is in accordance with theoretical expectations [*Rundle et al.*, 2000, Figure 4].

[19] We note here that the minimum b value of the magnitude distributions that we generate is 0.75. This lies within the lower range of observed b values 0.7–1.3 [*Frohlich and Davis*, 1993]. In practice, because of the upper magnitude truncations introduced by (6) or (7), the actual b values of the simulated catalogs are usually larger (see section 5). We also note that the particular implementation of the stress release model used here does not include aftershocks, and that aftershock removal from natural catalogs leads to an apparent decrease in the observed b value [*Frohlich and Davis*, 1993].

4. Experimental Design

[20] Within the formulation outlined above, there remain several factors which may influence the occurrence of ASR. Briefly, these are whether (and possibly how) the average event size increases with the level $X(t)$ of the process; whether the event rate increases with the level; and how decreases in the level scale with event size.

[21] Firstly, let us consider the form of the dependence (on the level $X(t)$) of the equivalent magnitude γ, and thus the average event size. Figure 3 of *Weatherley et al.* [2000] shows that the maximum size of simulated events from a cellular automaton model increases with the model stress. If we bin model events according to stress level at their time of occurrence, and fit the resulting frequency-size distribution following (6) or (7), we obtain the estimated M_c and $m_{\max}$ as a function of model energy (read "stress") as shown in Figure 1.

[22] In Figure 1 is it clear that M_c and $m_{\max}$ increase as a function of the model system energy at failure. For the tapered Pareto distribution the two nonlinear functions have the smallest RMS error and capture the apparent curvature in the distribution better. Thus we will model the change

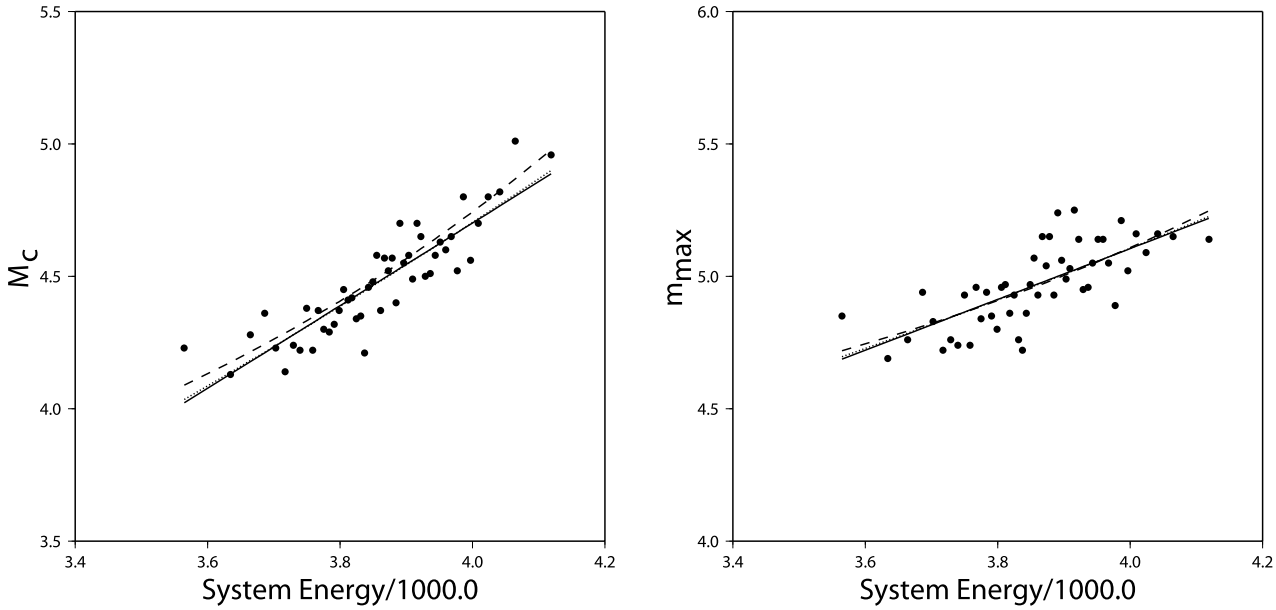

Figure 1. An illustration of how the large magnitude tail (M_c or $m_{\max}$) of the distribution may depend upon system energy. The cumulative frequency magnitude (defined as $\log_{10}$ event energy release) distributions of 10,000 events (binned by system energy at failure) from the cellular automaton model studied by *Jaumé et al.* [2000] and *Weatherley et al.* [2000] were fit to the tapered Pareto (left: (6)) and truncated Gutenberg-Richter (right: (7)) distributions. Lines represent linear (solid), exponential (dashed), and power-law (dotted; $u_2 = 2.0$ in (10)) fits to the relationship between M_c or $m_{\max}$ and the system energy at failure. For (6) the exponential fit has the smallest RMS error, followed by the power-law fit, and then the linear fit. For (7) the power-law fits best, followed by the linear and exponential fits.

in γ with the level $X(t)$ using those two possibilities; exponential,

$$\gamma = u_0 + u_1 e^X, \tag{9}$$

and power-law dependence,

$$\gamma = u_0 + u_1 (1 + X_+)^{u_2}, \tag{10}$$

where the subscript + denotes the positive part. As a check, we can also consider the invariant case with $\gamma = 7.0$. Taking the magnitude range of interest for the accelerating events as $M \geq 5.0 = u_0$ [*Jaumé and Sykes*, 1999], some experimentation established that the process was sufficiently stable to produce lengthy output catalogs, which appear to satisfactorily mimic observed seismic records, with $u_1 = 0.1$ and $u_2 = 2.0$ in (9) and (10). For the truncated Gutenberg-Richter distribution, values of $u_0 = 6.0$, $u_1 = 0.2$, $u_2 = 2.0$ produced similarly satisfactory catalogs. When using the truncated Gutenberg-Richter distribution, greater care had to be exercised concerning the choice of the parameters u_0 and u_1 than with the tapered Pareto distribution. Otherwise, the abrupt truncation of the distribution resulted in output catalogs noticeably different from observed catalogs. This manifested in two ways: either the distribution had a "turn up" following the "turn down," or had a sharp truncation. In neither case was ASR observed, although some sort of "cycles" were clearly present in the former. We note that other parameterizations of the relationship between $X(t)$ and γ are possible (see section 6).

[23] Secondly, there is the question of whether the rate of events should increase with the level $X(t)$ as in (4), which might possibly naturally result in ASR without the necessity of increasing the average event size. The alternative of setting $\lambda(t)$ = constant results in a Poisson process, which would require that γ remains level-dependent, and that the level $X(t)$ continue to evolve following (3).

[24] Finally, there is the question of whether the quantity accumulated in the level of the process should be Benioff strain or seismic moment [see *Imoto*, 2001; *Bebbington and Harte*, 2003]. In the former case, the stress release is calculated by [*Benioff*, 1951; *Gutenberg and Richter*, 1956]

$$S_i = \epsilon_i = 10^{2.4+0.75M_i} \tag{11}$$

and in the latter case by [*Hanks and Kanamori*, 1979]

$$S_i = E_i = 10^{9.0+1.5M_i}. \tag{12}$$

[25] We are now in a position to perform a series of simulation experiments to examine the effects of the factors enumerated above. For each meaningful combination of factors a sequence of approximately 10,000 events was produced and examined for ASR sequences using the methodology of *Jaumé et al.* [2000].

[26] The simulation procedure is relatively straightforward and proceeds as follows:

[27] 1. Using a variant of the Shedler-Lewis thinning method [*Lewis and Shedler*, 1976; *Ogata*, 1981] we generate the time of the next event using the time-varying

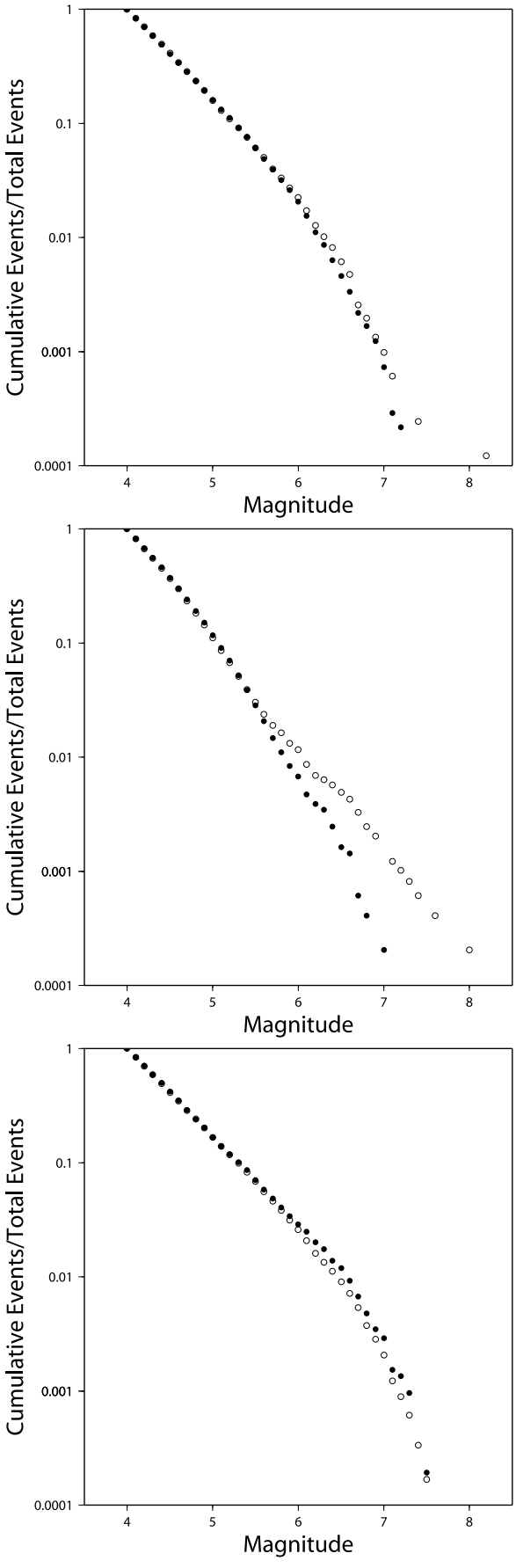

intensity $\lambda(t)$ in (4). Note that $X(t)$ increases between events, and so this is simpler if $\lambda(t)$ is a constant.

[28] 2. We then generate a strain release from the distribution (5) or (7), using in the former case the fact [*Vere-Jones et al.*, 2001] that the distribution is the minimum of an exponential and a Pareto random variable. The thresholds y_0 and m_0 are set such that the resulting magnitude distribution has $M_{\min} = 4.0$, i.e., a unit below the minimum turning point. The parameter γ ($m_{\max}$ for the truncated Gutenberg-Richter) can depend on the level $X(t)$ at the event time through (9) or (10), or be constant.

[29] 3. This strain release is then converted into a magnitude via (8).

[30] 4. The level $X(t)$ is then reduced by an amount (11) or (12) depending on whether it corresponds to accumulated Benioff strain or seismic moment, respectively.

[31] 5. After reducing $X(t)$ by the generated amount, we find the next event time.

5. Simulation Results

[32] In the case when the intensity $\lambda(t)$ was constant, the resulting magnitude distributions did not appear to be of modified Gutenberg-Richter form (Figure 2, middle), due to the mixing over γ [cf. *Vere-Jones et al.*, 2001, section 3.2]. However, in all cases where (4) was used, the output distributions were of modified Gutenberg-Richter form (Figure 2, top, bottom). In allowing both $\lambda(t)$ and γ to be dependent on the level, the fact that lower $X(t)$ values are associated with fewer events through (4) further mixes the observed distribution. The output catalogs had b values ranging from 0.75 to 0.92, consistent with the choice of $\alpha = 1$ above.

[33] A total of 16 simulated catalogs were produced (Table 2), eight using each of the tapered Pareto and truncated Gutenberg-Richter distributions. For each catalog two analyses were run on each model output: one where M_{main} was selected so as to have 10 or more events with $M \geq M_{main}$ and a second with M_{main} such that there were 25 or more events with $M \geq M_{main}$. Examination of the time intervals between these terminating events produced coefficients of variation (standard deviation/mean) ranging from 0.59 to 0.90, apart from Models 6, 12 and 14, with coefficients of variation 1.63, 1.62 and 2.25 respectively. These latter signal the possibility of rare, very large, events which reduce $X(t)$ to a very low level. These are presumably possible in all of the models simulated, although the effect would not be as noticeable in the models with constant λ, or as frequent in the models with constant γ. Overall, our simulated sequences appear to have a satisfactory degree of irregularity.

Figure 2. Aggregated magnitude-frequency distributions resulting from stress release model simulations using the tapered Pareto magnitude-frequency distribution. (top) Simulations where both λ and γ are dependent on X. (middle) Simulations where λ is constant and only γ depends on X. (bottom) Simulations where γ is constant and only λ depends on X. Solid circles, models using $S_i = 10^{2.4+0.75M_i}$ (strain); open circles, models using $S_i = 10^{9.0+1.5M_i}$ (moment).

Table 2. Model Parameters and Results of ASR Analysis

Model	FM[a]	$\lambda(t)$	γ	X[b]	M_{main}[c]	%model[d]	%random[e]
1A[f]	TP	$e^{\mu+\nu X}$	7.0	strain	7.2	43	47
1B[g]	TP	$e^{\mu+\nu X}$	7.0	strain	7.0	51	63
2A	TP	$e^{\mu+\nu X}$	7.0	moment	7.0	60	57
2B	TP	$e^{\mu+\nu X}$	7.0	moment	6.7	75	48
3A	TP	const.	$5 + u_1 e^X$	strain	6.4	27	18
3B	TP	const.	$5 + u_1 e^X$	strain	6.0	33	34
4A	TP	const.	$5 + u_1 e^X$	moment	6.9	80	33
4B	TP	const.	$5 + u_1 e^X$	moment	6.4	58	31
5A	TP	$e^{\mu+\nu X}$	$5 + u_1 e^X$	strain	6.9	24	35
5B	TP	$e^{\mu+\nu X}$	$5 + u_1 e^X$	strain	6.7	33	48
6A	TP	$e^{\mu+\nu X}$	$5 + u_1 e^X$	moment	6.8	69	40
6B	TP	$e^{\mu+\nu X}$	$5 + u_1 e^X$	moment	6.6	70	50
7A	TP	$e^{\mu+\nu X}$	$5 + u_1(1 + X_+)^{u_2}$	strain	7.0	43	58
7B	TP	$e^{\mu+\nu X}$	$5 + u_1(1 + X_+)^{u_2}$	strain	6.8	41	52
8A	TP	$e^{\mu+\nu X}$	$5 + u_1(1 + X_+)^{u_2}$	moment	6.8	83	33
8B	TP	$e^{\mu+\nu X}$	$5 + u_1(1 + X_+)^{u_2}$	moment	6.6	81	58
9A	TGR	$e^{\mu+\nu X}$	7.5	strain	7.4	47	59
9B	TGR	$e^{\mu+\nu X}$	7.5	strain	7.3	52	41
10A	TGR	$e^{\mu+\nu X}$	7.5	moment	7.4	60	20
10B	TGR	$e^{\mu+\nu X}$	7.5	moment	7.2	70	48
11A	TGR	const.	$6 + u_1 e^X$	strain	7.0	33	42
11B	TGR	const.	$6 + u_1 e^X$	strain	6.7	55	45
12A	TGR	const.	$6 + u_1 e^X$	moment	7.0	73	36
12B	TGR	const.	$6 + u_1 e^X$	moment	6.5	57	54
13A	TGR	$e^{\mu+\nu X}$	$6 + u_1 e^X$	strain	7.4	36	57
13B	TGR	$e^{\mu+\nu X}$	$6 + u_1 e^X$	strain	7.2	32	64
14A	TGR	$e^{\mu+\nu X}$	$6 + u_1 e^X$	moment	7.4	77	31
14B	TGR	$e^{\mu+\nu X}$	$6 + u_1 e^X$	moment	7.1	70	33
15A	TGR	$e^{\mu+\nu X}$	$6 + u_1(1 + X_+)^{u_2}$	strain	7.5	15	77
15B	TGR	$e^{\mu+\nu X}$	$6 + u_1(1 + X_+)^{u_2}$	strain	7.3	35	54
16A	TGR	$e^{\mu+\nu X}$	$6 + u_1(1 + X_+)^{u_2}$	moment	7.4	82	27
16B	TGR	$e^{\mu+\nu X}$	$6 + u_1(1 + X_+)^{u_2}$	moment	7.1	66	31

[a]Frequency-magnitude distribution used to create simulated catalogs; TP, tapered Pareto; TGR, truncated Gutenberg-Richter.
[b]Decrease in X from an event of magnitude M equals $10^{0.75M+2.4}$ (strain); $10^{1.5M+9.0}$ (moment).
[c]Mainshock magnitude cutoff used in analysis.
[d]Percent of mainshocks from the stress release model with $C < 0.7$.
[e]Percent of mainshocks from randomized catalog with $C < 0.7$.
[f]Analysis using M_{main} with 10 or more events.
[g]Analysis using M_{main} with 25 or more events.

[34] The seismic strain release $\Omega(t)$ in the time period between earthquakes with $M \geq M_{main}$ was fitted to (1), constrained by the t_f and $\Omega(t_f)$ of the mainshock. Only those events with magnitudes within 2.0 units of the mainshock magnitude M were used to calculate $\Omega(t)$, consistent with empirical practice [*Jaumé and Sykes*, 1999]. The fit to (1) was determined, following *Bowman et al.* [1998], by minimizing

$$C = \frac{\text{power-law RMS}}{\text{linear RMS}},$$

where "power-law RMS" refers to the least squares fit to (1) and "linear RMS" is that of the best-fitting least squares straight line to $\Omega(t)$, premainshock ($t < t_f$). The B, m, and t in (1) that produced the smallest value of C was taken as the best fit; A in (1) is constrained to be $\Omega(t_f)$. However, t was restricted to be between 0.1 and 10.0 of the mean interevent time between events with $M \geq M_{main}$ and m was restricted to vary between 0.0 and 0.8, to insure that the best fit would have at least a minimum amount of curvature. *Bowman et al.* [1998] use a threshold of $C < 0.7$ as being indicative of ASR behavior. Figure 3 shows an example of the fit to the simulated seismicity before the second mainshock in Model 2A.

[35] In order to establish a benchmark for the presence or absence of ASR in our simulated catalogs, we also randomized the event times in the simulated catalogs and reanalyzed them in the same fashion. The randomization was accomplished by generating a set of random numbers (one for each event in the simulated catalog) and mapping them onto the same time window as the simulated catalog. The events were then resorted into sequential time order. The percentage of fits with $C < 0.7$ in these randomized catalogs is also shown in Table 2.

[36] On the basis of the percentage of $M \geq M_{main}$ events with $C < 0.7$, the models analyzed fall into two major groups. Those models where the level $X(t)$ is accumulated Benioff strain generally have few (24–51%) mainshock events where the preceding seismicity follows (1). Conversely, those models where $X(t)$ is accumulated seismic moment have a larger (58–83%) percentage of mainshock sequences that follow (1). In the randomized catalogs, some 18–63% of the large event sequences exhibit ASR, overlapping the results where Benioff strain is used as $X(t)$. In all models using seismic moment as $X(t)$ the randomized catalogs contain fewer apparent ASR sequences than the original (unrandomized) catalogs; in all but one model using Benioff strain as $X(t)$ the randomized catalogs contain more apparent ASR sequences than the unrandomized catalogs.

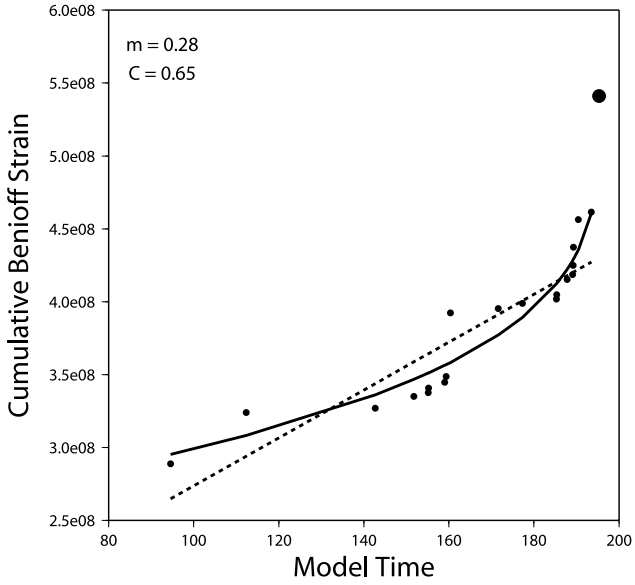

Figure 3. The fit (solid line) to (1) for the cumulative strain release (solid circles, earthquake events; large circle, mainshock) prior to the second mainshock in Model 2A. The least squares (dashed line) linear fit is also shown. *m* is the exponent in (1), and *C* is the *Bowman et al.* [1998] curvature parameter.

We must conclude that ASR is present in the former case, and absent in the latter. Our results using the truncated Gutenberg-Richter frequency-magnitude distribution parallel those using tapered Pareto. ASR occurs most frequently when $X(t)$ is seismic moment (57–82%), least frequently when it is Benioff strain (15–55%), with results from the randomized catalogs falling in between (20–77%).

[37] We also analyzed the simulated catalogs using variations on the constraints defined above, such as allowing $\Omega(t_f)$ to be a variable to be fitted and using events of all sizes to define $\Omega(t)$. As expected, this resulted in a different set of percentages of good fits to (1). However, we find the separation of results into two groups based upon whether seismic moment or Benioff strain is used as $X(t)$ is a very robust feature of the simulated catalogs. If anything, the variations in fitting constraints outlined at the start of this paragraph lead to an even more extreme separation of results into two groups, compared to the conservative constraints used to produce Table 2.

[38] Within the group of models with accumulated seismic moment as the level $X(t)$, it is a model having both the event rate $\lambda(t)$ and the upper turning magnitude γ dependent on the level (Model 8) which yields the largest percentage of ASR sequences (81–83%). In the other models approximately two-thirds (57–82%) of the mainshocks are preceded by ASR sequences.

6. Discussion

[39] As signposted in section 1, we also performed the search for ASR sequences in the simulated catalogs using seismic moment as $\Omega(t)$, using the same constraints and fitting procedure as for Benioff strain. We find that none of the models produce more than 60% apparent ASR sequences. In general, using seismic moment as $\Omega(t)$ reduces the percentage of good fits to (1) in both the stimulated catalogs and their randomized equivalents; i.e., in 43 of the 44 cases in Table 2 where the percentage is >40%, using seismic moment reduces the number of good fits. It may be that (1) is simply not an accurate description of the evolution of cumulative seismic moment release, and may explain in part why Benioff strain is the empirically preferred quantity.

[40] A major assumption underlying the work described here is that there is some relationship between a state variable of the earthquake system and the rate and/or size distribution of the resulting events. This view has both historical roots in earthquake seismology [e.g., *Reid*, 1910; *Shimazaki and Nakata*, 1980] and has been bolstered by recent results from simulation models of earthquake systems [e.g., *Steacy and McCloskey*, 1998; *Ben-Zion et al.*, 2003]. We expect that further analysis from a variety of earthquake simulation models may suggest other possible parameterizations for the dependence, on the level $X(t)$, of the upper turning magnitude γ and perhaps the rate $\lambda(t)$.

[41] Our results suggest that, at least in the variants of the stress release model studied here, it is how decreases in the level of the process $X(t)$ are apportioned between events of different magnitude that determines whether or not ASR behavior is observed. In our simulations the *b* value at lower magnitudes is approximately 0.75, so if the level $X(t)$ corresponds to accumulated Benioff strain, most of the "stress release" is concentrated in the smaller magnitudes (Figure 4). Conversely, when accumulated seismic moment is used as the level, most of the "stress release" is in the larger magnitudes (Figure 4). This is also why the choice of parameters is more sensitive when using the truncated

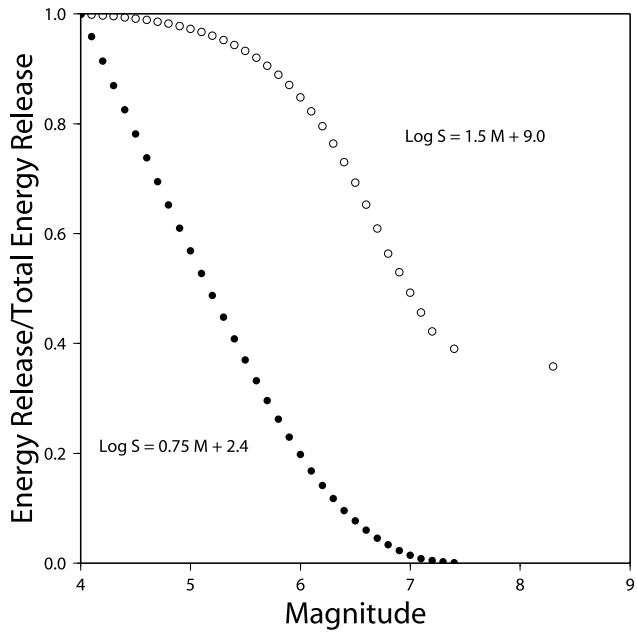

Figure 4. Proportion of energy released as a function of magnitude in two of the simulation models. The identity of S_i largely controls whether energy is primarily released in smaller versus larger events. Solid circles, Model 5 (Benioff strain); open circles, Model 6 (seismic moment).

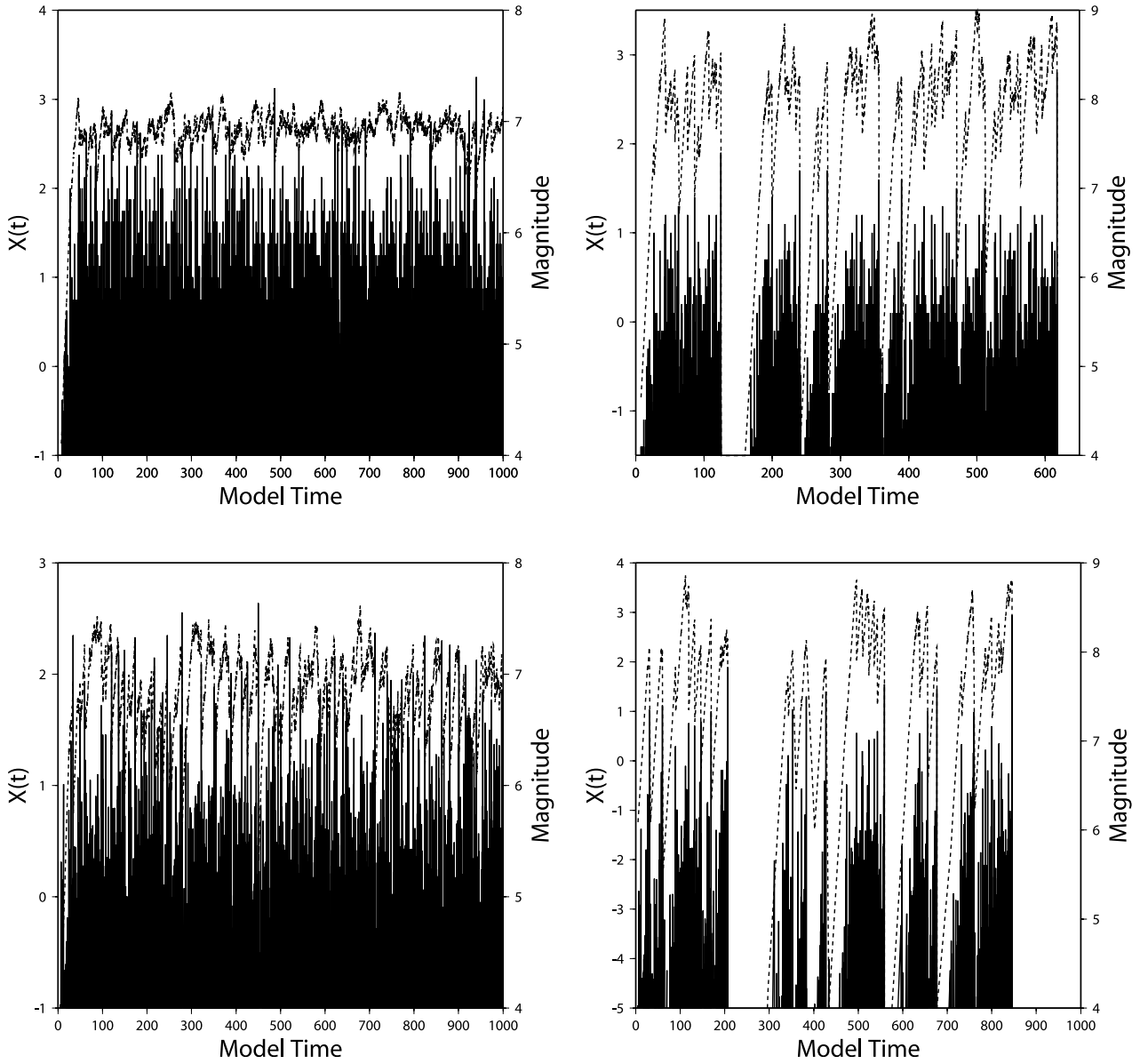

Figure 5. Evolution of state vector X(t) (dashed line) and earthquake occurrence (vertical lines) during stress release model simulations. Note that the entire simulated catalogs are not shown. Top row: Models using the tapered Pareto distribution. (left) Model 5 (Benioff strain). (right) Model 6 (seismic moment). Bottom row: Models using the truncated Gutenberg-Richter distribution. (left) Model 13 (Benioff strain). (right) Model 14 (seismic moment).

Gutenberg-Richter distribution. The effect of the system level has to be sufficient to overcome the sharp truncation of the magnitude distribution. This results in an output catalog of tapered Pareto form.

[42] Figure 5 shows typical temporal behavior of the stress release model. With accumulated Benioff strain as $X(t)$, we see that perturbations are small, and hence so are the variations in rate and average size of events. This is a characteristic of "self-organizing criticality" (SOC) behavior, rather than the "intermittent criticality" implicit in ASR. However, with accumulated seismic moment as $X(t)$ we see that the system can be "discharged" from time to time, with consequent delays until the rate of events, and/or their average size, can again noticeably accelerate. The differing time axes between the left and right panels of Figure 5 reflect this behavior; i.e., a magnitude 8+ event in Model 6 at model time 617 "shuts down" the simulated seismicity and events (of magnitude $> m_0$) do not begin again until much later (not shown). Similar behavior occurs at model time 845 in Model 14 (Figure 5). Because of the different regimes controlling the underlying level $X(t)$ in these models, the rate of events in model time is quite different. However, as is obvious from (4), model time can be scaled by multiplying the parameters to equalize this. Hence we simply sought to produce simulated catalogs with roughly equal numbers of events.

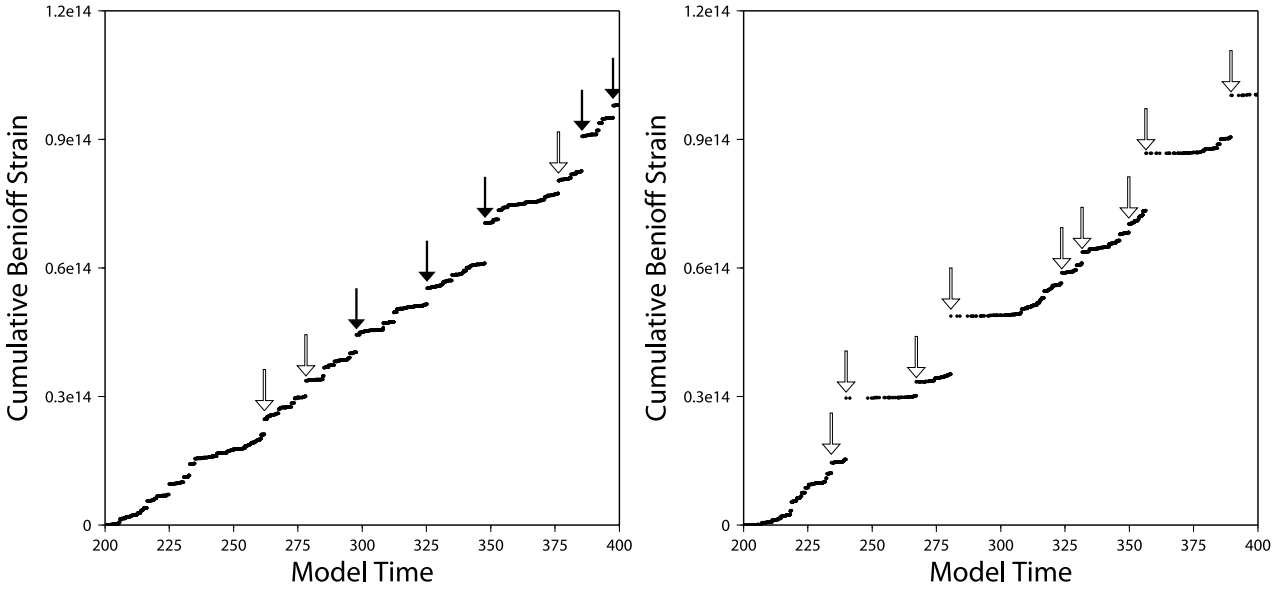

Figure 6. Cumulative Benioff strain release during 200 time step segments of Models 5 and 6. Arrows mark mainshock events (open, premainshock Benioff strain release fits (1); filled, premainshock Benioff strain release does not fit (1)). (left) Model 5 (Benioff strain). (right) Model 6 (seismic moment).

[43] Figure 5 also illustrates the cause underlying the difference in behaviors. If $X(t)$ is accumulated seismic moment then the stress release of the small events are small enough relative to their mean that, in spite of the small drops, $X(t)$ continues to trend upward. Hence the rate $\lambda(t)$ and/or the upper turning magnitude γ continue to increase, until a large enough event occurs to ''terminate'' the sequence. Thus the pattern of cumulative seismic release $\Omega(t)$ (2) is quite ''cyclic,'' and many ASR sequences are observed. On the other hand, if $X(t)$ is accumulated Benioff strain, then the stress release of the small events are larger relative to their mean, and a sequence can be ''terminated'' by several small events as well as by a large one. Hence the record appears more regular in terms of seismic release than an ASR pattern, and few ASR sequences are observed (Figure 6). In fact the latter case produces fewer ASR sequences than random chance, indicating that the stress release model using accumulated Benioff strain models ASR poorly.

[44] Our results bear considerable similarity to those from a variety of cellular automaton simulations [*Sammis and Smith*, 1999; *Jaumé et al.*, 2000; *Weatherley et al.*, 2000]. ASR sequences do not occur in conservative automata with uniform cell sizes, but are produced in nonconservative cellular automata and those with fractal cell size distributions [*Sammis and Smith*, 1999]. *Jaumé et al.* [2000] find ASR sequences in heterogeneous cellular automata with a crack-like stress redistribution law that leaves the previously ruptured cells stress free after an event [*Steacy and McCloskey*, 1998] but not in an automaton which redistributes significant stress to previously ruptured cells [*Steacy and McCloskey*, 1999]. What unites these observations and our results is that ASR sequences occur in those models in which large events produce significant energy level drops in the overall system.

[45] It is relevant here to remember that a prediction from one of the ''approach to criticality'' models of ASR is that it arises from an increase in the upper turning magnitude γ. This results in an increase in the number and size of events in the large event tail of the observed distribution [*Rundle et al.*, 1999]. *Jaumé* [2000] tested this prediction by examining the difference in earthquake magnitude-frequency distributions during the first and second halves of 17 known ASR sequences, finding that the change in the magnitude-frequency distributions for 15 of these sequences was consistent with the model of *Rundle et al.* [1999]. We have similarly analyzed the output magnitude-frequency distributions within the ASR sequences of Model 4. The comparison with the results of *Jaumé* [2000] is shown in Figure 7.

[46] We see that the stress release model produces changes in the magnitude-frequency distribution similar to natural cases; if anything the natural variation is less than that seen in the simulation model. Of course, in a simulation model, we have no missed observations.

[47] The results are not sensitive to the choice of m_0 = 4.0. For computational purposes, we require only that this cutoff be at least two magnitudes less than the magnitude of the event being examined as a candidate for the end of an ASR sequence. Since the lower part of the magnitude distribution is pure Gutenberg-Richter, including still smaller events in our catalogs, and hence in the level $X(t)$, would tend only to accentuate our results. However, this is tied to the exclusion of aftershocks from our model. The stress release model is capable of producing realistic aftershock sequences through augmentation by stress transfer to a secondary process [*Borovkov and Bebbington*, 2003]. However, this requires a number of additional parameters. Because of the magnitude cutoffs used here, which are typical of ASR studies, the aftershocks would not materially affect the results, and so the mainshock only model was used in order to aid comprehension. The b values of the simulated catalogs are consistent with this.

[48] Having demonstrated that our simple stochastic model is capable of producing repeated instances of ASR

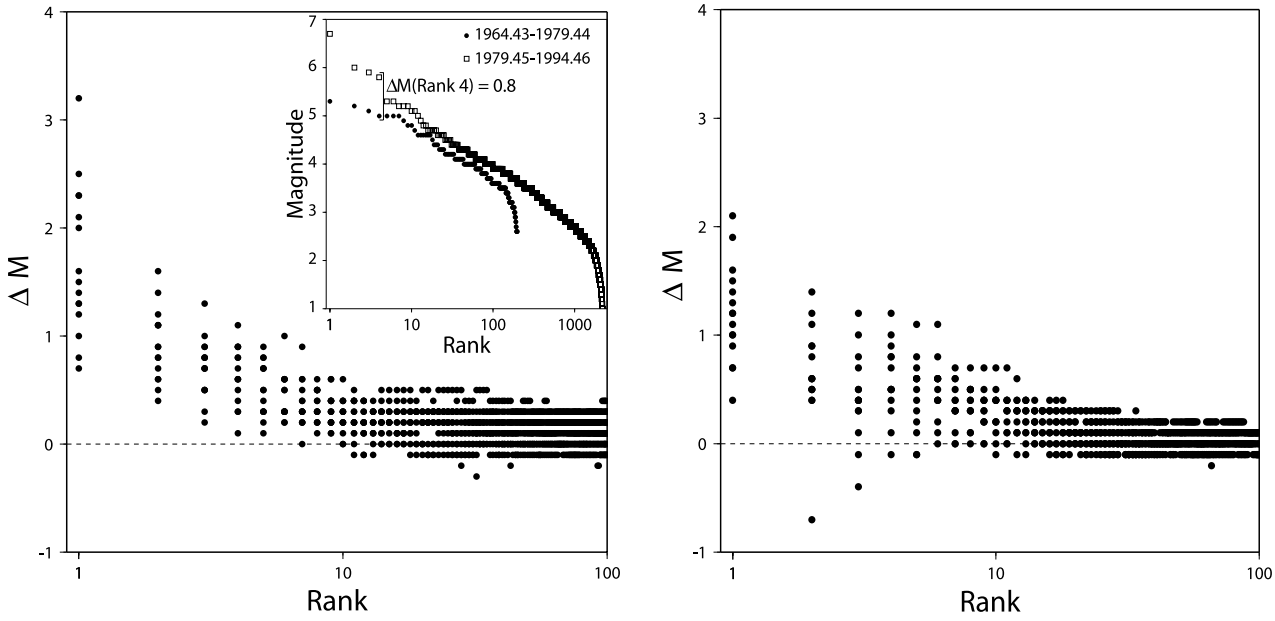

Figure 7. Change in magnitude distributions during first versus second halves (based upon time) of ASR sequences. Earthquakes are ranked by magnitude, and the difference in magnitude between the distributions is plotted as a function of rank (inset on left shows construction for ASR sequence associated with 1994 $M = 6.7$ Arthur's Pass, New Zealand earthquake, modified from Figure 2 of *Jaumé* [2000]). (left) Fifteen natural ASR cases (Figure 10a, *Jaumé*, 2000). (right) Fifteen simulated sequences from Model 4 that have $C < 0.7$. The large ΔM at small rank indicates that the largest events occur during the latter half of the ASR sequence. Figures 2 and 10a from *Jaumé* [2000].

(as well as SOC behavior), the next step will be to develop a method for fitting the parameters in the conditional intensity (4) and the size distribution (5). Taking the intensity and the size distribution separately, the former can be fitted by standard point process maximum likelihood methods [*Daley and Vere-Jones*, 2003, section 7.2], while *Kagan and Schoenberg* [2001] have examined a number of estimators for the parameter(s) of the tapered Pareto distribution. However, we need to fit them simultaneously, a far more difficult problem. It appears that the only feasible way in which the marked (by magnitude) point process as a whole can be fitted to data will be through a Bayesian framework. While *Tsapanos et al.* [2001] outline a Bayesian approach to estimating parameters in the truncated Gutenberg-Richter law, *Rotondi and Varini* [2004] indicate that simultaneously fitting this law and the stress release process parameters requires Monte Carlo methods to compute the required Bayesian distributions.

7. Conclusions

[49] We have developed an extension of the stress release model which can reproduce many aspects of ASR sequences observed in earthquake catalogs. In this model we find that the presence or absence of ASR is largely dependent on the scaling of the effect of the event magnitudes on the internal level of the process. Variants where either or both of the earthquake occurrence rate and the upper "cutoff" of the earthquake size distribution are dependent on the level of the process, produce a significant percentage of simulated ASR sequences only when the level of the process corresponds to accumulated seismic moment. We have also verified that, in these simulations, the frequency-magnitude distributions evolve in similar fashion to that in observed cases of ASR (see Figure 7 and its discussion). This suggests that self-correcting type models are an effective tool for developing methods of parameter estimation and hazard forecasting using ASR, through the generation of large synthetic catalogs, and by providing an alternative fitting methodology for cross-checking of ASR forecasts.

[50] **Acknowledgments.** This work was supported by the Marsden fund, administered by the Royal Society of New Zealand. We thank David Vere-Jones, Kostya Borovkov, and Rick Schoenberg for valuable discussions. Karen Felzer, an anonymous referee, and an associate editor suggested much-needed improvements in exposition. This research was facilitated by the hospitality of the Institute of Mathematics and its Applications during the "Mathematics in the Geosciences" program.

References

Bebbington, M., and D. Harte (2003), The linked stress release model for spatio-temporal seismicity: Formulations, procedures and applications, *Geophys. J. Int.*, *154*, 925–946.

Benioff, H. (1951), Earthquakes and rock creep, Part 1: Creep characteristics of rocks and the origin of aftershocks, *Bull. Seismol. Soc. Am.*, *41*, 31–62.

Ben-Zion, Y., M. Eneva, and Y. Liu (2003), Large earthquake cycles and intermittent criticality on heterogeneous faults due to evolving stress and seismicity, *J. Geophys. Res.*, *108*(B6), 2307, doi:10.1029/2002JB002121.

Bird, P., Y. Y. Kagan, and D. D. Jackson (2000), Frequency-magnitude distribution, effective lithosphere thickness, and seismic efficiency of oceanic transforms and spreading ridges, *Eos Trans. AGU*, *81*(22), West. Pac. Meet. Suppl., Abstract S51H-01.

Bowman, D. D., G. Ouillon, C. G. Sammis, D. Sornette, and A. Sornette (1998), An observational test of the critical earthquake concept, *J. Geophys. Res.*, *103*, 24,359–24,372.

Borovkov, K., and M. S. Bebbington (2003), A stochastic two-node stress transfer model reproducing Omori's law, *Pure Appl. Geophys.*, *160*, 1429–1445.

Bufe, C. G., and D. J. Varnes (1993), Predictive modeling of the seismic cycle in the greater San Francisco Bay region, *J. Geophys. Res.*, *98*, 9871–9883.

Burroughs, S. M., and S. F. Tebbens (2002), The upper-truncated power law applied to earthquake cumulative frequency-magnitude distributions: Evidence for a time-independent scaling parameter, *Bull. Seismol. Soc. Am.*, *92*, 2983–2993.

Daley, D. J.. and D. Vere-Jones (2003), *An Introduction to the Theory of Point Processes*, 2nd ed., vol. 1, 464 pp., Springer-Verlag, New York.

Frohlich, C., and S. D. Davis (1993), Teleseismic b values; or much ado about 1.0, *J. Geophys. Res.*, *98*, 631–644.

Geller, R. J., D. D. Jackson, Y. Y. Kagan, and F. Mulargia (1997), Earthquakes cannot be predicted, *Science*, *275*, 1616–1617.

Gutenberg, B., and C. F. Richter (1956), Earthquake magnitude, intensity, energy and acceleration, *Bull. Seismol. Soc. Am.*, *46*, 105–145.

Hanks, T. C., and H. Kanamori (1979), A moment magnitude scale, *J. Geophys. Res.*, *84*, 2348–2350.

Imoto, M. (2001), Application of the stress release model to the Nankai earthquake sequence, Southwest Japan, *Tectonophysics*, *338*, 287–295.

Jaumé, S. C. (2000), Changes in earthquake size-frequency distributions underlying accelerating seismic moment/energy release, in *Geocomplexity and the Physics of Earthquakes*, *Geophys. Monogr. Ser.*, vol. 120, edited by J. B. Rundle, D. L. Turcotte, and W. Klein, pp. 199–210, AGU, Washington, D. C.

Jaumé, S. C., and L. R. Sykes (1999), Evolving towards a critical point: A review of accelerating seismic moment/energy release prior to large and great earthquakes, *Pure Appl. Geophys.*, *155*, 279–305.

Jaumé, S. C., D. K. Weatherley, and P. Mora (2000), Accelerating seismic energy release and evolution of event time and size statistics: Results from two heterogeneous cellular automaton models, *Pure Appl. Geophys.*, *157*, 2209–2226.

Kagan, Y. Y. (1991), Seismic moment distribution, *Geophys. J. Int*, *106*, 123–134.

Kagan, Y. Y. (1994), Observational evidence for earthquakes as a nonlinear dynamic process, *Phys. D*, *77*, 160–192.

Kagan, Y. Y. (1997), Seismic moment-frequency relationship for shallow earthquakes: Regional comparisons, *J. Geophys. Res.*, *102*, 2835–2852.

Kagan, Y. Y. (2002), Seismic moment distribution revisited: I. Statistical results, *Geophys. J. Int.*, *148*, 520–541.

Kagan, Y. Y., and F. Schoenberg (2001), Estimation of the upper cutoff parameter for the tapered Pareto distribution, *J. Appl. Probab.*, *38A*, 158–175.

Lewis, P. A. W., and G. S. Shedler (1976), Simulation of non-homogeneous Poisson processes with loglinear rate function, *Biometrika*, *63*, 501–506.

Main, I. G. (1999), Applicability of time-to-failure analysis to accelerated strain before earthquakes and volcanic eruptions, *Geophys. J. Int.*, *139*, F1–F6.

Mora, P., D. Place, S. Abe, and S. Jaumé (2000), Lattice solid simulation of the physics of fault zones and earthquakes: The model, results and directions, in *Geocomplexity and the Physics of Earthquakes*, *Geophys. Monogr. Ser.*, vol. 120, edited by J. B. Rundle, D. L. Turcotte, and W. Klein, pp. 105–125, AGU, Washington, D. C.

Ogata, Y. (1981), On Lewis' simulation method for point processes, *IEEE Trans. Inform. Theory*, *IT-30*, 23–31.

Reid, H. F. (1910), The mechanism of the earthquake, in *The California Earthquake of April 18, 1906, Report of the State Earthquake Investigation Commission*, vol. 2, pp. 1–192, Carnegie Inst., Washington, D. C.

Rotondi, R., and E. Varini (2004), Bayesian analysis of a marked point process: Application in seismic hazard assessment, *Stat. Methods Appl.*, in press.

Rundle, J. B., W. Klein, and S. Gross (1999), Physical basis for statistical patterns in complex earthquake populations: Models, predictions and tests, *Pure Appl. Geophys.*, *155*, 575–607.

Rundle, J. B., W. Klein, D. L. Turcotte, and B. D. Malamud (2000), Precursory seismic activation and critical phenomena, *Pure Appl. Geophys.*, *157*, 2165–2182.

Sammis, C. G., and S. W. Smith (1999), Seismic cycles and the evolution of stress correlation in cellular automaton models of finite fault networks, *Pure Appl. Geophys.*, *155*, 307–334.

Shimazaki, K., and T. Nakata (1980), Time-predictable recurrence model for large earthquakes, *Geophys. Res. Lett.*, *7*, 279–282.

Sornette, D., and C. G. Sammis (1995), Complex critical exponents from renormalization group theory of earthquakes: Implications for earthquake prediction, *J. Phys. I France*, *5*, 607–619.

Sornette, D., and A. Sornette (1999), General theory of the modified Gutenberg-Richter law for large seismic moments, *Bull. Seismol. Soc. Am.*, *89*, 1121–1130.

Steacy, S. J., and J. McCloskey (1998), What controls an earthquake size? Results from a heterogeneous cellular automaton, *Geophys. J. Int.*, *133*, F11–F14.

Steacy, S. J., and J. McCloskey (1999), Heterogeneity and the earthquake magnitude-frequency distribution, *Geophys. Res. Lett.*, *26*, 899–902.

Tsapanos, T. M., A. A. Lyubushin, and V. F. Pisarenko (2001), Application of a Bayesian approach for estimation of seismic hazard parameters in some regions of the Circum-Pacific Belt, *Pure Appl. Geophys.*, *158*, 859–875.

Varnes, D. J. (1989), Predicting earthquakes by analyzing accelerating precursory seismic activity, *Pure Appl. Geophys.*, *130*, 661–686.

Vere-Jones, D. (1978), Earthquake prediction: A statistician's view, *J. Phys. Earth*, *26*, 129–146.

Vere-Jones, D., R. Robinson, and W. Yang (2001), Remarks on the accelerated moment release model: Problems of model formulation, simulation and estimation, *Geophys. J. Int.*, *144*, 517–531.

Weatherley, D., S. Jaumé, and P. Mora (2000), Evolution of stress deficit and changing rates of seismicity in cellular automaton models of earthquake faults, *Pure Appl. Geophys.*, *157*, 2183–2207.

Zheng, X., and D. Vere-Jones (1991), Applications of stress release models to earthquakes from North China, *Pure Appl. Geophys.*, *135*, 559–576.

Zheng, X., and D. Vere-Jones (1994), Further applications of the stochastic stress release model to historical earthquake data, *Tectonophysics*, *229*, 101–121.

M. S. Bebbington, IIS&T, Massey University, Private Bag 11222, Palmerston North, New Zealand. (m.bebbington@massey.ac.nz)

S. C. Jaumé, Department of Geology and Environmental Geosciences, College of Charleston, 66 George Street, Charleston, SC 29424, USA. (jaumes@cofc.edu)